ANTIMICROBIAL AGENTS AND CHEMOTHERAPY, June 2006, p. 2156–2166 Vol. 50, No. 6
0066-4804/06/$08.00+0 doi:10.1128/AAC.01499-05

Functional, Biophysical, and Structural Bases for Antibacterial Activity of Tigecycline

Matthew W. Olson,[1]†‡ Alexey Ruzin,[2]†* Eric Feyfant,[3]† Thomas S. Rush III,[3]§ John O'Connell,[2] and Patricia A. Bradford[2]

Department of Chemical and Screening Sciences, Wyeth Research, Pearl River, New York 10965[1]; Department of Infectious Disease, Wyeth Research, Pearl River, New York 10965[2]; and Departments of Computational Chemistry and Structural Biology, Wyeth Research, Cambridge, Massachusetts 02140[3]

Received 21 November 2005/Returned for modification 20 January 2006/Accepted 9 March 2006

Tigecycline is a novel glycylcycline antibiotic that possesses broad-spectrum activity against many clinically relevant species of bacterial pathogens. The mechanism of action of tigecycline was delineated using functional, biophysical, and molecular modeling experiments in this study. Functional assays showed that tigecycline specifically inhibits bacterial protein synthesis with potency 3- and 20-fold greater than that of minocycline and tetracycline, respectively. Biophysical analyses demonstrated that isolated ribosomes bind tigecycline, minocycline, and tetracycline with dissociation constant values of 10^{-8}, 10^{-7}, and $>10^{-6}$ M, respectively. A molecular model of tigecycline bound to the ribosome was generated with the aid of a 3.40-angstrom resolution X-ray diffraction structure of the 30S ribosomal subunit from *Thermus thermophilus*. This model places tigecycline in the A site of the 30S subunit and involves substantial interactions with residues of H34 of the ribosomal subunit. These interactions were not observed in a model of tetracycline binding. Modeling data were consistent with the biochemical and biophysical data generated in this and other recent studies and suggested that tigecycline binds to bacterial ribosomes in a novel way that allows it to overcome tetracycline resistance due to ribosomal protection.

Glycylcyclines are novel semisynthetic compounds that contain a glycylamido substitution at position 9 of various tetracycline derivatives (27, 28). Tigecycline (Fig. 1), the 9-*t*-butylglycylamido derivative of minocycline, is an expanded broad-spectrum antibiotic that is not affected by classical tetracycline resistance mechanisms including ribosomal protection and efflux by tetracycline-specific pumps (3, 7, 20, 21). Tigecycline, the first-in-class glycylcycline currently approved in the United States for the treatment of complicated intra-abdominal and skin infections, is in development worldwide. In vitro and in vivo studies have shown that tigecycline is effective against drug-resistant gram-positive and gram-negative bacteria (5, 18–21).

An abundance of data has been generated on the antimicrobial activity of tigecycline and on the mechanisms of decreased susceptibility to tigecycline (4, 9, 12, 14, 20, 25, 26, 30). However, only three biochemical studies were performed with tigecycline and other glycylcyclines. It was previously shown that glycylcyclines were significantly more potent inhibitors than tetracycline and possessed fivefold-greater affinity for the ribosome (2, 23). By using Fe^{2+}-mediated cleavage, Bauer et al. showed that tigecycline bound to the same high-affinity site as tetracycline in the 16S rRNA (1). However, the data suggested that tigecycline bound in a different orientation and with greater affinity than tetracycline. In addition, mutational analyses confirmed the binding site for tigecycline where a decrease in tigecycline susceptibility was observed with *Escherichia coli* strains with known mutations in the A site (either G966U or G1058C) in the rRNA. Although these studies provided qualitative insights, a quantitative evaluation describing the biophysical binding of tigecycline to the ribosome relative to other compounds was not fully elucidated.

To this end, a series of experiments were performed to further characterize the mode of action of tigecycline. First, the inhibition of protein synthesis was demonstrated with an in vitro translation assay. Second, the equilibrium binding constants for tigecycline, minocycline, and tetracycline were determined and confirmed by both functional and compound competition assays. Finally, the nature of the interaction of tigecycline with the A site of the 16S rRNA of the ribosome was computationally probed relative to tetracycline to provide insights into structural activity relationships at the molecular level.

* Corresponding author. Mailing address: Wyeth Research, Department of Infectious Disease, 401 North Middletown Road, Bldg. 200, Rm. 3218, Pearl River, NY 10965. Phone: (845) 602-4592. Fax: (845) 602-5671. E-mail: ruzina@wyeth.com.

† These authors contributed to this work equally.

‡ Present address: Johnson & Johnson Pharmaceutical Research & Development, 665 Stockton Drive, Exton, PA 19341.

§ Present address: Department of Medicinal Chemistry, Merck Research Laboratories, 33 Avenue Louis Pasteur, Boston, MA 02115.

MATERIALS AND METHODS

Chemicals. Compounds used in this study were obtained from the following sources: tigecycline and ^{14}C-labeled tigecycline (0.2 Ci/mmol) from Wyeth Research, Pearl River, NY; tetracycline, minocycline, and rifampin from Sigma Chemical Co., St. Louis, MO. Uridine 5′-[α-^{33}P]triphosphate (^{33}P-α-UTP; 3,000 Ci/mmol), ^{3}H-labeled tetracycline (1 Ci/mmol), and Microscint-20 were obtained from Perkin-Elmer, Wellesley, MA. Dithiothreitol (DTT), MgOAc, Tris base, NaCl, KCl, EDTA, $MgCl_2$, 2-mercaptoethanol. and NH_4Cl were purchased

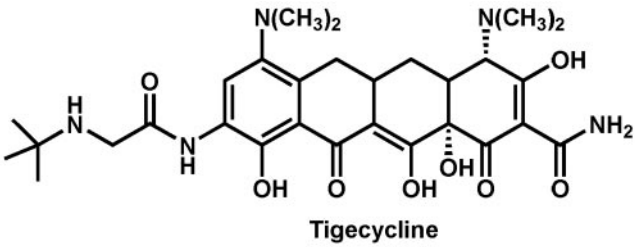

FIG. 1. Structure of tigecycline.

from Research Organics, Cleveland, OH. Protease inhibitors were purchased from Roche Applied Science, Indianapolis, IN. HEPES (pH 7.5) was purchased from Gibco-BRL/Invitrogen, Carlsbad, CA. Coomassie Protein Plus reagent and bovine serum albumin (BSA) were purchased from Pierce Chemical Company, Rockford, IL.

IVT assay. In vitro transcription/translation (IVT) reactions were performed by using the RTS 100 *E. coli* HY kit (Roche Applied Science, Penzberg, Germany) as specified by the manufacturer. Radiolabeled green fluorescent protein (GFP) was synthesized by using a GFP plasmid vector (pIVEX control vector GFP, part of the kit) as a DNA template and L-[^{35}S]methionine (Amersham, Piscataway, NJ) as the source of ^{35}S. A typical IVT sample (12.5 μl) contained 3 μl of *E. coli* lysate (part of the kit), 2.5 μl of reaction mix, 3 μl of amino acid solution, 0.625 μl of 1 mM methionine, 1 μl of L-[^{35}S]methionine (15 μCi), 1.25 μl of reconstitution buffer, 0.125 μl of Milli-Q water, 0.5 μl of either Milli-Q water or compound solution, and 0.5 μl of either Milli-Q water or GFP vector (0.125 μg). Following the addition of compounds, samples were preincubated for 5 min at 30°C and then supplied with GFP vector and incubated for 1 h at 30°C. An aliquot (0.5 μl) of each sample was mixed with 19 μl of Laemmli sample buffer (Bio-Rad, Hercules, CA), loaded on a 12.5% Tris-HCl Criterion gel (Bio-Rad), and separated by sodium dodecyl sulfate-polyacrylamide gel electrophoresis at constant voltage (120 V) as described previously (13). Following electrophoresis, the gel was washed in Milli-Q-water for 20 min, dried on 3MM paper (Whatman, Cambridge, United Kingdom), and exposed to a phosphor storage screen (Bio-Rad) for 4 h. Qualitative and quantitative data acquisition was performed by phosphorimagery using the Bio-Rad Molecular Imager FX

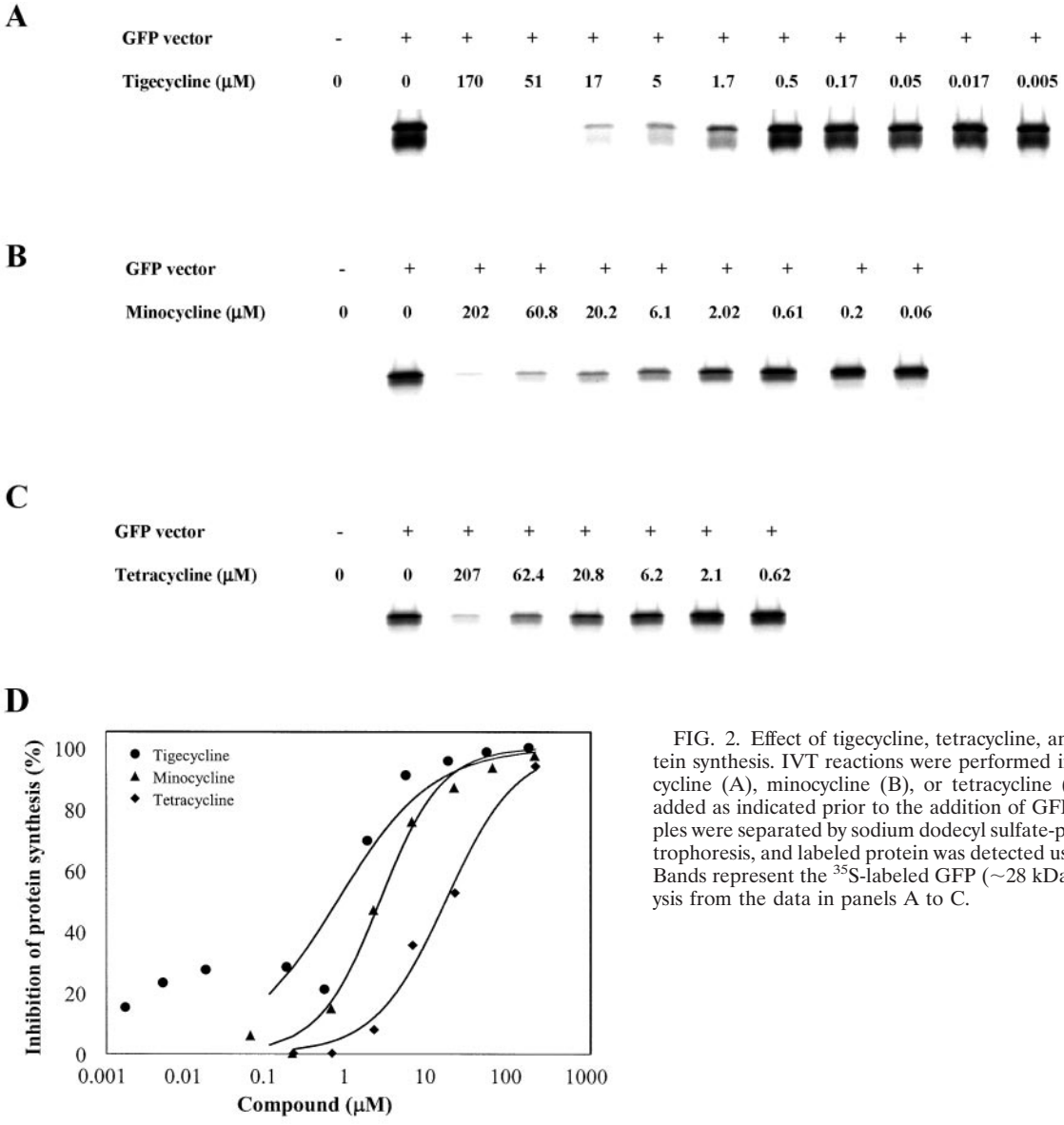

FIG. 2. Effect of tigecycline, tetracycline, and minocycline on protein synthesis. IVT reactions were performed in the presence of tigecycline (A), minocycline (B), or tetracycline (C). Compounds were added as indicated prior to the addition of GFP plasmid vector. Samples were separated by sodium dodecyl sulfate-polyacrylamide gel electrophoresis, and labeled protein was detected using a phosphorimager. Bands represent the ^{35}S-labeled GFP (~28 kDa). (D) IC_{50} value analysis from the data in panels A to C.

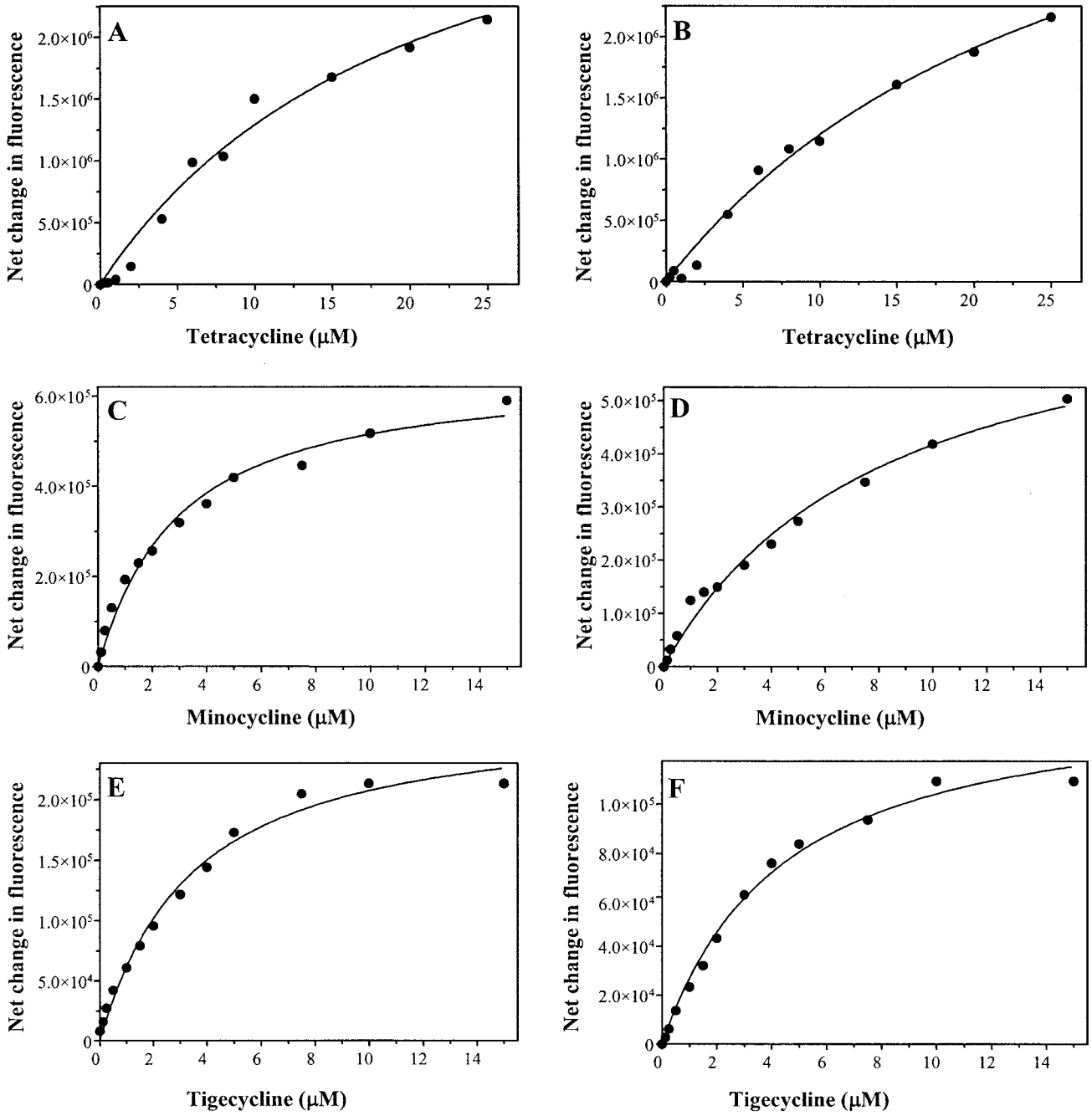

FIG. 3. Binding isotherms for the interactions of tigecycline, minocycline, and tetracycline with 30S and 70S ribosomes where compound is titrated into the system. The isolated 30S (A, C, and E) and 70S (B, D, and F) ribosomes were incubated with tetracycline (A and B), minocycline (C and D), and tigecycline (E and F). Samples contained 1.5 μM of ribosomes for tetracycline and 0.5 μM for tigecycline and minocycline. The net change in fluorescence for tigecycline, minocycline, and tetracycline was measured at 515 to 520 nm, 505 to 510 nm, and 515 to 520 nm, respectively, in the presence of increasing concentrations of compound: 0 to 25 μM tetracycline, 0 to 15 μM tigecycline, and 0 to 15 μM minocycline. The solid line in each panel corresponds to the curve fit to the quadratic equation.

system and Quantity One 4.1.1 software (Bio-Rad). Data were quantitated by volume integration of the expressed GFP in each lane. Fifty percent inhibitory concentration (IC_{50}) values for inhibition of protein synthesis were determined from the following equation: % inhibition = 100 × (volume mm^2 of signal − volume mm^2 background)/(volume mm^2 max − volume mm^2 background). Signal is the integrated volume in the presence of compound, background is the integrated volume of an area corresponding to a reaction that did not contain the GFP vector, and max is the integrated volume of a reaction performed in the absence of compound. From these data, the IC_{50} value for each compound was determined by a sigmoid dose-response (variable slope, model 35) using LSW data analysis (MDL Software) and the equation $y = (B_{max} * x\hat{}n)/(K\hat{}n + x\hat{}n)$ where y = response or percent inhibition, n = Hill slope, x = logarithm of concentration of compound, and K = IC_{50} value with B_{max} constrained to be 100.

TABLE 1. Equilibrium binding constants for tetracycline, minocycline, and tigecycline binding to the *E. coli* 30S and 70S ribosomes where compound was titrated into the system

Compound	K_D value (μM)	
	30S ribosome	70S ribosome
Tetracycline	19.7[a]	26[a]
Minocycline	2.6	7.8[a]
Tigecycline	3.1	3.9

[a] These equilibrium binding constants are K_D apparent (K_{Dapp}) values, as complete saturable binding was not achieved.

Ribosome purification. *E. coli* [DH5α F$^-$ ϕ80d*lacZ*Δ*M15* Δ(*lacZYA-argF*)*U169 recA1 endA1 hsdR17*(r_K^- m_K^+) *phoA supE44* λ$^-$ *thi-1 gyrA96 relA1*] was fermented to mid-log phase in F medium supplemented with 1% glucose (8). Bacterial cells were resuspended in an equal weight/volume of 20 mM Tris (pH 7.5) and 10% sucrose, flash frozen in liquid nitrogen, and stored at −20°C. Ribosomes were isolated from 38 g of *E. coli* essentially as described by Kiel et al. (11) and Moazed (17). DTT and protease inhibitors were added to all buffers (used according to the manufacturer's instructions), and HEPES (pH 7.5) was substituted for Tris (pH 7.5). *E. coli* DH5α was lysed with a French pressure cell (12,500 lb/in^2) at 3 g cells/ml, and the ribosomes were separated on a 10 to 30% sucrose gradient by centrifugation for 15 h at 22,000 rpm in an SW28 rotor. Ribosome concentration was determined by both A_{260} and protein assay (Coomassie Protein Plus reagent and BSA as the standard, according to the manufacturer's instructions).

Fluorescence binding studies. Fluorescent spectroscopic methods were used to determine the binding potency of tetracycline, minocycline, and tigecycline for the purified 30S and 70S ribosomes as a function of both compound and ribosome concentration. To ensure compound stability, 10 mM stocks of each compound were made fresh and used within 3 h. The molar extinction coefficients for tetracycline, minocycline, and tigecycline were determined in 5 mM MgOAc and were ε_{378} = 19,400, 33,500, and 27,200 · M^{-1} · cm^{-1}, respectively. The changes in the quantum yield and emission maximum of each compound were monitored. The intrinsic fluorescence of each compound was monitored with a Jobin-Yvon Horiba fluorometer (Fluoromax-3). The polarized emission spectra were obtained with vertically polarized excitation at 380 nm; the emission range was 480 to 560 nm. Fluorometric measurements were performed at 25°C in 5- × 5-mm quartz cells in 20 mM HEPES (pH 7.5), 5 mM MgOAc, 50 mM NH_4Cl, and 0.1 mM DTT. All buffer components were sterilized by filtration through an 0.2-μm nitrocellulose filter (Corning, Corning, NY) prior to use. All fluorescent spectra were scanned in the ratio mode (signal/reference) to compensate for variations in lamp output as a function of wavelength. Fluorescence was monitored 5 min after addition of the ribosome solution to the quartz cell. The excitation and emission bandwidths used were 2 nm and 8 nm for tigecycline, 2 nm and 4 nm for minocycline, and 2 nm and 2 nm for tetracycline, respectively. Where binding was monitored as a function of compound concentration, the isolated 30S and 70S ribosomes were present at 0.5 μM for tigecycline and minocycline and 1.5 μM for tetracycline. Compound was then titrated into the solution (0.5 ml) from 0.125 to 15 μM for tigecycline and minocycline and from 0.125 to 25 μM for tetracycline. Where binding of compound was monitored as a function of ribosome concentrations, the isolated 30S and 70S ribosomes were titrated into a 1 μM (0.5-ml) solution of each compound and fluorescence intensity increase was monitored. For tigecycline and minocycline, the 30S and 70S ribosomes were titrated from 0 to 7 μM. For tetracycline, the 30S and 70S ribosomes were titrated from 0 to 14 μM and 0 to 9 μM, respectively. Equilibrium binding constants were determined by using nonlinear curve fitting and a quadratic algorithm, $Y = F^*[(X + P_t + K_D) - (\{[(P_t + X + K_D)^2] - (4^*X^*P_t)\}^{0.5})]/(2^*P_t)$, within the program Graphpad Prism, where Y is change in fluorescence intensity, X is fluorophore concentration, P_t is protein concentration, K_D is dissociation constant, and F is fluorescence intensity at saturation. The binding was considered as saturable when the K_D value obtained was at least fourfold lower than the highest concentration of ligand evaluated in the assay.

Competition assays. The 30S (40 pmol, 0.8 μM) and 70S (70 pmol, 1.4 μM) ribosomes were added to a mixture of a fixed amount of [^{3}H]tetracycline (6 μM final concentration) and [^{14}C]tigecycline (4 μM final concentration) and various concentrations of unlabeled tetracycline, minocycline, and tigecycline (0 to 200 μM final concentration) in a final volume of 50 μl. The 30S binding reaction buffer contained 10 mM Tris (pH 8), 20 mM $MgCl_2$, 200 mM NaCl, 0.1 mM EDTA, and 6 mM 2-mercaptoethanol. The 70S binding reaction buffer contained 10 mM Tris (pH 8), 20 mM $MgCl_2$, 50 mM KCl, 0.1 mM EDTA, and 6 mM 2-mercaptoethanol. The reaction mixtures were incubated for 15 min at 37°C with mixing, and the samples were subjected to vacuum filtration over a Millipore Multiscreen-IP plate (0.45-μm pore size) and washed seven times with ice-cold binding buffer. The filters were allowed to dry, and the bound radioactivity was determined by scintillation counting in a Wallac MicroBeta after the addition of 60 μl of Microscint-20. Quantitation (pmol of compound bound) was achieved by determining the specific activity of the radiolabel by spotting 2 μl of the binding reaction mixture onto the filter plate and then adding scintillant and counting as above. The data provided allow one to calculate a value for cpm-pmol^{-1} in the reaction mixture and thereby the number of pmol compound bound. EC_{50} values (concentration required to achieve 50% reduction in the amount of radiolabeled compound bound to ribosome) were determined by using LSW data analysis (MDL Software) and the following equation: 100 × (pmol of signal − pmol background)/(pmol max − pmol background), where signal is the quantity (pmol) of radiolabeled compound bound to the ribosome in the presence of unlabeled compound, background is the quantity (pmol) of radiolabeled compound retained on the filter in the absence of ribosome, and max is the quantity (pmol) of ligand bound to the ribosome and retained on the filter in the absence of unlabeled compound.

Computational docking studies. Several molecular modeling software packages were used in this study to dock the ribosome ligands and evaluate system energetics. These included FLO (Thistlesoft Software Co.) to explore possible ribosome-ligand binding modes, Sybyl (Tripos Inc.) for system and site-based minimizations, Macromodel (Schrodinger Inc.) to explore ligand conformations and energies, and Zap_Bind (OpenEye Scientific Software, Inc.) to calculate solvation-based electrostatics.

The A site of the 3.4-angstrom X-ray diffraction structure (Protein Data Bank code 1HNW) (6) was used as the receptor site in this study. Prior to use, however, all hydrogens were added, a molecular mechanics-based minimization of the energy of the system was performed (in Sybyl using the MMFF94 force field), and then all small molecules were removed to leave an empty, minimized, chemically competent binding site for docking. The minimization of the site and of tetracycline was necessary to adjust the structural parameters to the energy function that was used for the binding experiment and, in addition, to correct some discrepancies between the Protein Data Bank structure and the description of the binding poses of tetracycline as shown in the original article by Brodersen et al. (6).

The binding pose of tetracycline (the one found after minimization of 1HNW) and the area surrounding its site of interaction were the primary focus of our efforts. The binding mode for minocycline was extrapolated by modifying tetracycline to minocycline and minimizing, whereas binding modes for tigecycline were explored using FLO and its "mcdock" procedure with the surrounding protein side chains and nucleic acid bases left flexible; all other atoms were fixed. The mcdock procedure utilizes a Monte Carlo sampling and docking technique, which is described in more detail by Brodersen et al. (6). Energetic evaluations (docking scores) are based on a combined MM3 and AMBER molecular mechanics force field (15), which was modified to include parameters specific for this system (e.g., Mg ion parameters). Several of the best-scoring binding modes per ligand were saved and evaluated further (see below).

The FLO-generated poses were then subjected to final Sybyl-based minimizations and rescoring using energy terms derived from Sybyl, Macromodel, and Zap_Bind. The form of this final scoring function closely resembles that of one previously described MM-PBSA (molecular mechanics Poisson-Boltzmann/surface area) (24, 31) and is represented by the equation $E_{total} = E^g_{vdw} + E_{elec} + E_{hydro} + E_{rotors} + E^g_{int}$. This function not only includes the gas-phase energetics of interaction between the ribosome and ligand but also includes the effects of solvation. Here, E^g_{vdw} is the gas-phase van der Waals energy (Sybyl), E_{elec} is the Poisson-based electrostatics energy (screened Coulombic + desolvation; from Zap_Bind), E_{hydro} is a surface area-based approximation of the hydrophobic effect (Zap_Bind), E_{rotors} is a penalty representing the ligand's torsional entropy loss, and E^g_{int} is the ligand internal strain energy (Macromodel). Minimizations immediately prior to evaluation of the individual terms were performed in Sybyl using the MMFF94 force field and a distance-dependent Coulombic function with a dielectric constant of 4.

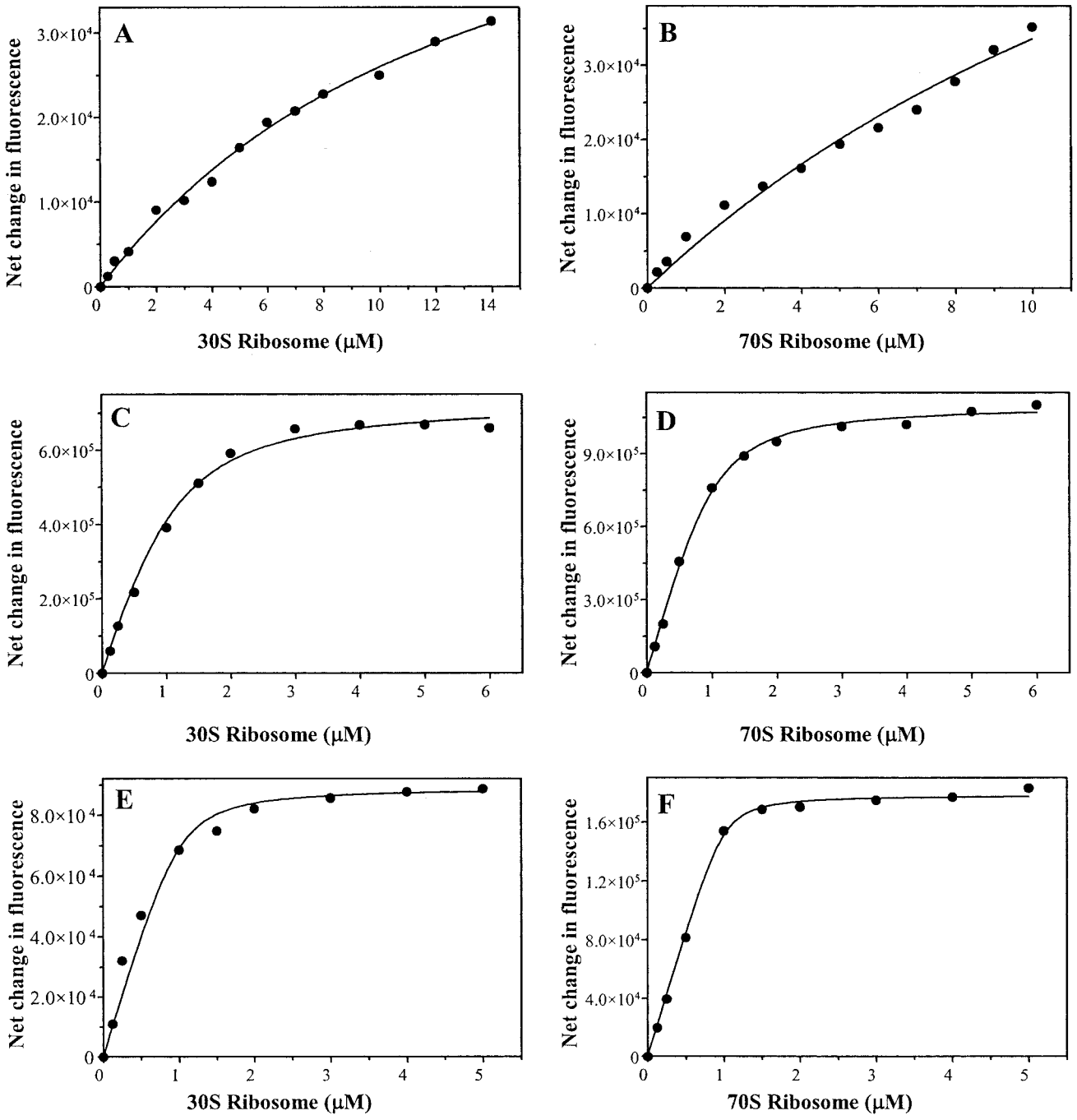

FIG. 4. Binding isotherms for the interactions of tigecycline, minocycline, and tetracycline with 30S and 70S ribosomes where ribosome is titrated into the system. Tigecycline (A and B), minocycline (C and D), and tetracycline (E and F) were present at 1 μM concentrations whereby the isolated 30S (A, C, and E) and 70S (B, D, and F) ribosomes were titrated into the system. The net change in fluorescence for tigecycline, minocycline, and tetracycline was measured at 510 to 520 nm, 505 to 515 nm, and 510 to 520 nm, respectively, in the presence of increasing concentrations of ribosome. The solid line in each panel corresponds to the curve fit to the quadratic equation.

RESULTS

Effect of tigecycline, tetracycline, and minocycline on protein synthesis. The structural similarity of tigecycline, tetracycline, and minocycline and the results of previous binding studies suggested that tigecycline, like tetracycline and minocycline, acts as an inhibitor of bacterial protein synthesis. Therefore, an IVT assay was employed to test this hypothesis. As shown in Fig. 2, each compound inhibited the synthesis of ^{35}S-GFP catalyzed by *E. coli* cell lysate. Calculated IC_{50} values for tigecycline, minocycline, and tetracycline were 0.75 ± 0.1 μM, 2.5 ± 0.25 μM, and 16.5 ± 3.3 μM, respectively. The multiple bands observed in Fig. 2 are likely due to overloading

TABLE 2. Equilibrium binding constants for tetracycline, minocycline, and tigecycline binding to the *E. coli* 30S and 70S ribosomes where the ribosome was titrated into the system

Compound	K_D value (μM)	
	30S ribosome	70S ribosome
Tetracycline	13.2[a]	19.6[a]
Minocycline	0.35	0.17
Tigecycline	0.07	0.03

[a] The equilibrium binding constants for tetracycline are K_D apparent (K_{Dapp}) values, as complete saturable binding was not achieved.

TABLE 3. Competition of [^{3}H]tetracycline binding to the *E. coli* 30S and 70S ribosomes by unlabeled tetracycline, minocycline, and tigecycline

Unlabeled compound[a]	EC_{50} (μM)	
	30S ribosome	70S ribosome
Tetracycline	7	4.9
Minocycline	1.4	0.6
Tigecycline	0.7	0.4

[a] Labeled compound ([^{3}H]tetracycline) was used at 6 μM final concentration.

of the sample, since the IVT reaction contains a host of reagents that might affect GFP migration in the gel. It should be noted that the tigecycline curve did not reach zero (Fig. 2D), which might suggest that in the functional assay tigecycline activity may be an underestimate and that even at nM concentrations the drug is effective at disrupting protein synthesis in this assay.

Binding of tigecycline, minocycline, and tetracycline to the 30S and 70S ribosomes. In addition to values provided by the functional assay, the potency of tigecycline, minocycline, and tetracycline was evaluated through determination of the equilibrium binding constants for each compound by monitoring their intrinsic fluorescence. Experiments were performed where either compound or ribosome was titrated into the assay. The titration of compound into the system

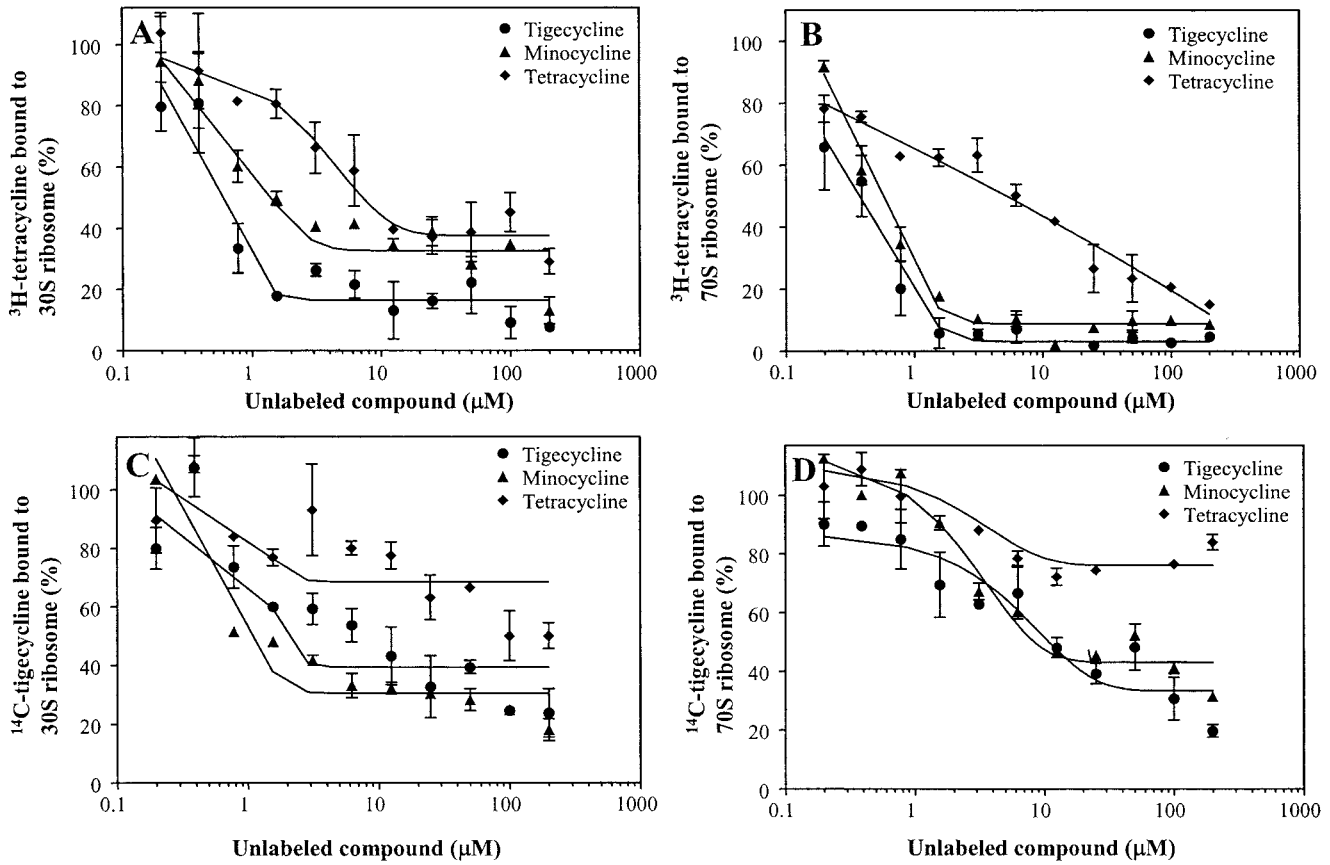

FIG. 5. Competition of [^{3}H]tetracycline and [^{14}C]tigecycline by unlabeled tigecycline, minocycline, and tetracycline. The 30S (40 pmol, 0.6 μM [A and C]) and 70S (70 pmol, 1.4 μM [B and D]) ribosomes were incubated for 15 min at 37°C with [^{3}H]tetracycline (6 μM [A and B]) or [^{14}C]tigecycline (4 μM [C and D]) in the presence of increasing concentrations of unlabeled tigecycline, minocycline, and tetracycline (0 to 200 μM). The quantity of [^{3}H]tetracycline and [^{14}C]tigecycline bound to the ribosomes was determined. For panels A to D, 100% binding represents the amount of radiolabeled compound bound in the absence of unlabeled compound. For panel A these values are 4, 4.5, and 4.7 pmol of [^{3}H]tetracycline for tigecycline, minocycline, and tetracycline titrated into the assay, respectively. Likewise for panel B these values are 4.2, 6.3, and 6.9 pmol, respectively. For panel C, the quantities of [^{14}C]tigecycline bound in the absence of unlabeled compound are 25, 34, and 30 pmol for tigecycline, minocycline, and tetracycline titrated into the system, respectively. Similarly for panel D, these values are 50, 64, and 58 pmol, respectively.

TABLE 4. Competition of [^{14}C]tigecycline binding to the *E. coli* 30S and 70S ribosomes by unlabeled tetracycline, minocycline, and tigecycline

Unlabeled compound[a]	EC_{50} (μM)	
	30S ribosome	70S ribosome
Tetracycline	ND[b]	ND
Minocycline	2	4.2
Tigecycline	2.5	5.5

[a] Labeled compound ([^{14}C]tigecycline) was used at 4 μM final concentration.
[b] ND, not determinable.

has the potential to detect multiple binding sites on the ribosome. This has been proposed for tetracycline, whereby a single high-affinity binding site and multiple (up to five) low-affinity binding sites exist (6, 22). In this study, binding of tigecycline, minocycline, and tetracycline was observed as a function of compound concentration (Fig. 3). The Hill coefficients for tetracycline, minocycline, and tigecycline binding to both the 30S and 70S ribosomes ranged from 1 to 1.3, indicating that no cooperative binding was observed. Saturable binding was observed to both 30S and 70S ribosomes for tigecycline (Fig. 3E and 3F) but only to 30S ribosome for minocycline (Fig. 3C). Saturable binding was not observed for tetracycline to either the 30S or the 70S ribosomes (Fig. 3A and 3B). It is likely that the inability to observe saturable binding for tetracycline (to both the 30S and 70S ribosomes) and minocycline (to the 70S ribosome) is due to the binding of tetracycline and minocycline to a lower-affinity binding site(s). The equilibrium binding constants for tigecycline and minocycline are similar, ranging from 3 to 8 μM, whereas for tetracycline these values are ca. 20 μM (Table 1).

The experimental design for the data in Fig. 4 and Table 2 is the reciprocal for the experiment shown in Fig. 3 and Table 1. Here, ribosome is titrated into the system, and as such, with compound limiting, binding should primarily occur at the high-affinity site, if the affinity for compound at the high-affinity site is sufficiently different from that at the low-affinity site(s). For both minocycline and tigecycline, saturable binding was observed at or near 1 μM concentrations of the 30S and 70S ribosomes (Fig. 4C to F). This is the same as the concentration of compound in the binding assay, which suggests stoichiometric binding of both tigecycline and minocycline at a high-affinity site. The K_D values for the 30S and 70S ribosomes are summarized in Table 2 and are on the order of 10^{-8} M, 10^{-7} M, and $>10^{-6}$ M for tigecycline, minocycline, and tetracycline, respectively.

Competition studies with [^{3}H]tetracycline and [^{14}C]tigecycline. To further confirm the data observed in the fluorescent binding assays, competition experiments were performed where radiolabeled tetracycline and tigecycline competed with unlabeled compounds for ribosome binding. In these competition studies, unlabeled and labeled compounds were given an equal opportunity to bind to the ribosome. As shown in Fig. 5A and 5B, both tigecycline and minocycline efficiently competed with [^{3}H]tetracycline for both 30S and 70S ribosomes. The EC_{50} values for tigecycline and minocycline were severalfold lower than the concentration of [^{3}H]tetracycline (Table 3). The results of the competition with [^{14}C]tigecycline are shown in Fig. 5C and 5D and Table 4. Although some competition was observed between tetracycline and [^{14}C]tigecycline, the EC_{50} values could not be determined even when tetracycline was used in a 50-fold molar excess over labeled compound. In contrast, both tigecycline and minocycline were able to compete with [^{14}C]tigecycline (EC_{50} values in 2 to 5.5 μM range).

Computational docking studies. Of the poses generated by computational modeling, there was one that was both energetically favorable and consistent with all known experimental information about the tigecycline-ribosome interaction (Fig. 6 and 7). Specifically, this binding pose scored well because of the favorable electrostatics and van der Waals and hydrogen-bonding interactions with atoms of the 30S subunit. This is in spite of the fact that none of the force fields used in this work specifically accounts for the enthalpic (quantum mechanical) interaction between the ligand and the surface-bound Mg. Compared to tetracycline, we found that tigecycline not only boasted more favorable van der Waals and Coulombic interactions but also a much lower desolvation penalty. Minocycline, on the other hand, was not as favorable as tigecycline in these areas but was found to have more favorable electrostatics than tetracycline (Fig. 6B).

Our model predicts that the tigecycline binding site intersects with that of the tetracyclines as shown in the X-ray structure. The most prominent commonalities between the ligand binding modes are (i) the coordination of a Mg ion that interacts with the phosphate groups of G1197, C1054, and U1196 and (ii) the proximity and close interactions between the A-ring substituents and G966, C1195, U1196, G1197, and G1198. However, what unequivocally separates the glycylcyclines from the tetracyclines is the fact that the glycylcyclines interact directly with other regions of the A site in a manner never seen before for any other class of A-site binding compounds. The first of these differences is the substantial hydrogen bonding interactions made between the aminoglycyl tail of tigecycline and C1054 in a *syn* orientation. The other major difference is in the additional contact/van der Waals interactions made by the *t*-butyl group with the irregular minor groove of H34 at or around the ribose ring of U1052, and the G530-A532 stretch of nucleotides on H18.

DISCUSSION

This study demonstrated that tigecycline specifically inhibits protein synthesis in an in vitro assay system containing the bacterial enzymes required for transcription and translation. Inhibition of protein synthesis by tigecycline was 3-fold more efficient than inhibition by minocycline and 20-fold more efficient than inhibition by tetracycline. This was consistent with previous work where glycylcyclines 9-(*N*,*N*-dimethylglycylamido)-minocycline (DMG-MINO), 9-(*N*,*N*-dimethylglycylamido)-6-demethyl-6-deoxytetracycline (DMG-DMDOT), and 9-(*N*,*N*-dimethylglycylamido)-doxycycline (DMG-DOX) inhibited bacterial protein synthesis with greater efficiency than did tetracycline and minocycline (2).

Biophysical binding experiments showed that tigecycline bound to the 30S and 70S ribosomes with 5-fold- and >100-fold-greater affinity than minocycline and tetracycline, respectively. These data were internally consistent with the potency differences in our functional assay. Previous work estimated

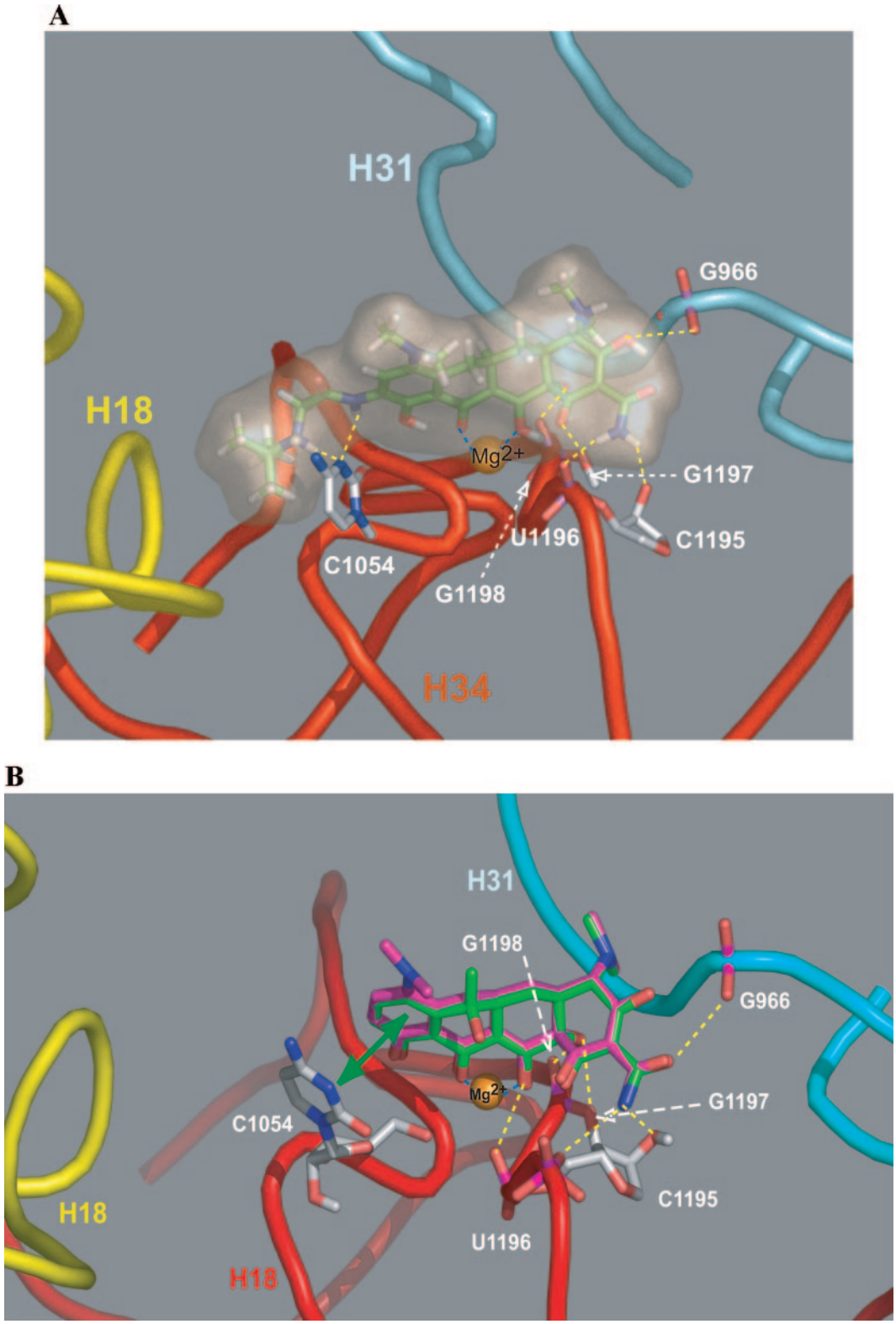

FIG. 6. Computational docking. A. Overview of the tigecycline binding site and the predicted ligand-ribosome interactions. The RNA helices H34, H31, and H18 are colored in red, cyan, and yellow, respectively. B. Overview of the tetracycline-ribosome interaction and the predicted minocycline-ribosome interactions. The RNA helices H34, H31, and H18 are colored in red, cyan, and yellow, respectively. Tetracycline is represented with its carbon atoms colored in green and minocycline with its carbon atoms colored in pink. The green double-headed arrow represents the π-stacking interaction between the D ring and the cytosine of C1054.

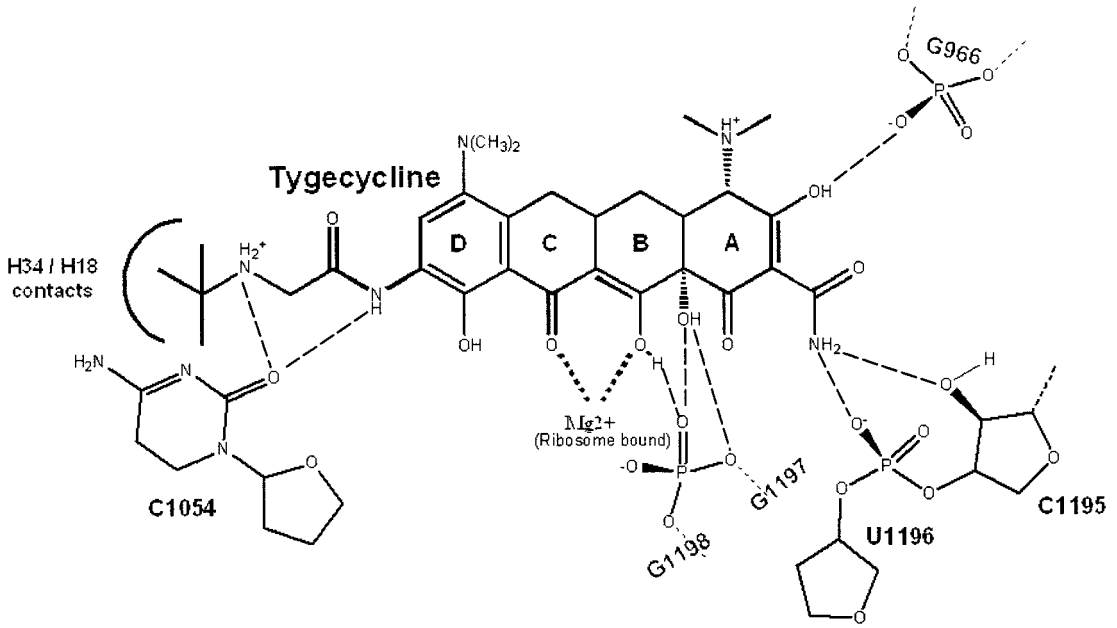

FIG. 7. Chemical structure diagram of the main interactions between tigecycline and the 16S RNA in the A binding site. The dashed lines represent the hydrogen bonds whereas the dotted lines represent the coordination bonds between tigecycline and a magnesium ion bound to the surface of the ribosome.

the K_D value for the tetracycline-ribosome interaction to be in the μM range (2, 10, 29). A comprehensive analysis by Tritton showed that tetracycline binds to a single strong binding site with an affinity of approximately 17 μM, which is in good agreement with the binding estimated in this study (29). Likewise, Bergeron et al. (2) estimated the K_D value to be as high as 10 μM for tetracycline binding to the 70S ribosome. The reason for the discrepancy between such a low-affinity experimental value for the tetracycline-ribosome interaction and the actual potency of the drug is not understood, which highlights certain limitations of in vitro experiments for direct estimation of in vivo activity of the compounds.

It should be noted that the K_D values describing the binding of tigecycline and minocycline to the 30S and 70S ribosomes where the ribosomes were titrated into the system were 1 to 2 logs lower than those where compound was titrated into the system. These data are consistent with the presence of a single high-affinity binding site and a separate low-affinity binding site(s) whereby the K_D values between the "high-" and "low-affinity" binding sites are significantly different. This observation was further supported by near-stoichiometric binding of tigecycline and minocycline to the 30S and 70S ribosome—presumably at the high-affinity site. In contrast, the affinity of tetracycline binding to the 30S and 70S ribosome was 10^{-5} M regardless of the method. This suggests that the K_D values for tetracycline binding to both the "high-" and "low-affinity" sites are not sufficiently different to allow for binding to the high-affinity site prior to binding to the lower-affinity site(s).

The results of competition experiments presented here are consistent with tigecycline and minocycline having greater affinity for both the 30S and 70S ribosomes. This study revealed that tigecycline competes for the 30S and 70S ribosome 10- to 12-fold more efficiently than tetracycline. Similarly, the relative affinities of DMG-DMDOT and DMG-DOX to the 70S ribosome were fivefold higher than that of tetracycline in a filter binding assay (2).

It has been suggested previously that tigecycline and tetracycline occupy the same or overlapping regions of the 16S RNA, but they appear to bind in unique orientations (1). A quantitative analysis by Bauer et al. (1) showed that the maximal signal increases for tigecycline and tetracycline for Fe^{2+}-mediated hydroxyl radical cleavage were at 1 and 100 μM, respectively. The 2-log reduction in tigecycline concentration required to bring about the same cleavage product by hydroxy radical footprinting is consistent with the functional and biophysical experiments in this report.

Biophysical studies with the tetracycline class of compounds led to the hypothesis that the compound effect of drugs that bind to the A site is due to the fact that they sterically prevent the binding of aminoacyl-tRNA during bacterial protein synthesis. The biophysical studies of Bauer et al. (1) and our energetically favorable A-site binding pose support the hypothesis that tigecycline shares this same mode of action. First, the Fe^{2+}-mediated hydroxyl radical cleavage experiments induced chain breakages at A964-A969, A1339-U1341, and C1195-A1197 in the presence of tetracycline and tigecycline (1). This result correlates with the X-ray experiment (31), where A964-A969 and C1195-A1197 were found to be part of the binding site for tetracycline. Our models, which also place tetracycline, minocycline, and tigecycline in the A site, show direct interactions with G966, C1195, and U1196. Second, C1054 is protected from dimethylsulfate-induced methylation in the presence of tigecycline (1). This is in agreement with our predicted binding mode since we find a strong interaction between the glycyl moiety of tigecycline and the base of C1054. This inter-

action, two hydrogen bonds, is very different from the one observed between C1054 and tetracycline (speculated to be a weaker π-type interaction). Finally, a shift in in vitro MICs of tigecycline is observed with the G966→U and G1058→C A-site mutations, which is consistent with the fact that G966 is specifically making interactions with tigecycline. For G1058, this base is not directly part of the A-binding site but just 3 nucleotides away. These studies suggest that the G1058 mutation affects the ligand-ribosome interactions around C1054. Further experiments, e.g., site-directed mutagenesis of position 1054, would be required to validate the predicted binding mode of tigecycline.

The computational modeling approach described in this study had the following limitations: (i) none of the force fields specifically accounted for the enthalpic (quantum mechanical) interaction between the ligand and the surface-bound Mg, as the coordination state cannot be reproduced by a typical mechanic force field, and (ii) the A binding site is a very large and mostly "flat" space completely open to solvent, suggesting that the solvent might be important in the binding of tigecycline, tetracycline, and minocycline; however, the role of the solvent can only be partially taken into account using the MM-PBSA scoring function used in this study.

As suggested previously, the ability of glycylcyclines to overcome TetM-mediated resistance could result from increased affinity of binding (23). Alternatively, it was also suggested that glycylcyclines might bind to the ribosome in a unique way that would render ribosomal protection by TetM ineffective. The data in this study support both possibilities, as tigecycline was seen to make additional strong contacts with nucleotides in H34 and H18, compared to tetracycline and minocycline. Nevertheless, the mechanism of ribosomal protection is not entirely understood. Presumably, binding of ribosomal protection proteins such as TetM and TetO alters ribosomal conformation and causes release of compounds such as tetracycline and minocycline (16). Perhaps tigecycline evades ribosomal protection due to either the stronger interactions or the unique mode of binding or a combination of the two factors. However, because the results of this study indicate that minocycline is comparable to tigecycline (albeit less efficient in inhibition of protein synthesis and ribosomal binding), it is likely that the additional interaction sites between tigecycline and ribosomes uncovered by the binding model presented in this study contribute substantially to the ability of tigecycline to overcome ribosomal protection and to maintain activity against tetracycline-resistant bacteria.

ACKNOWLEDGMENTS

We thank Steven Projan and Girija Krishnamurthy for discussions and suggestions regarding this work.

REFERENCES

1. **Bauer, G., C. Berens, S. J. Projan, and W. Hillen.** 2004. Comparison of tetracycline and tigecycline binding to ribosomes mapped by dimethylsulphate and drug-directed Fe^{2+} cleavage of 16S rRNA. J. Antimicrob. Chemother. **53:**592–599.
2. **Bergeron, J., M. Ammirati, D. Danley, L. James, M. Norcia, J. Retsema, C. A. Strick, W. G. Su, J. Sutcliffe, and L. Wondrack.** 1996. Glycylcyclines bind to the high-affinity tetracycline ribosomal binding site and evade Tet(M)- and Tet(O)-mediated ribosomal protection. Antimicrob. Agents Chemother. **40:**2226–2228.
3. **Boucher, H. W., C. B. Wennersten, and G. M. Eliopoulos.** 2000. In vitro activities of the glycylcycline GAR-936 against gram-positive bacteria. Antimicrob. Agents Chemother. **44:**2225–2229.
4. **Bouchillon, S. K., D. J. Hoban, B. M. Johnson, T. M. Stevens, M. J. Dowzicky, D. H. Wu, and P. A. Bradford.** 2005. In vitro evaluation of tigecycline and comparative agents in 3049 clinical isolates: 2001 to 2002. Diagn. Microbiol. Infect. Dis. **51:**291–295.
5. **Bradford, P. A.** 2004. Tigecycline: a first in class glycylcycline. Clin. Microbiol. Newsl. **26:**163–168.
6. **Brodersen, D. E., W. M. Clemons, Jr., A. P. Carter, R. J. Morgan-Warren, B. T. Wimberly, and V. Ramakrishnan.** 2000. The structural basis for the action of the antibiotics tetracycline, pactamycin, and hygromycin B on the 30S ribosomal subunit. Cell **103:**1143–1154.
7. **Chopra, I.** 2002. New developments in tetracycline antibiotics: glycylcyclines and tetracycline efflux pump inhibitors. Drug Resist. Updates **5:**119–125.
8. **Cull, M. G., and C. S. McHenry.** 1995. Purification of *Escherichia coli* DNA polymerase III holoenzyme. Methods Enzymol. **262:**22–35.
9. **Dean, C. R., M. A. Visalli, S. J. Projan, P. E. Sum, and P. A. Bradford.** 2003. Efflux-mediated resistance to tigecycline (GAR-936) in *Pseudomonas aeruginosa* PAO1. Antimicrob. Agents Chemother. **47:**972–978.
10. **Epe, B., and P. Woolley.** 1984. The binding of 6-demethylchlortetracycline to 70S, 50S and 30S ribosomal particles: a quantitative study by fluorescence anisotropy. EMBO J. **3:**121–126.
11. **Kiel, M. C., H. Aoki, and M. C. Ganoza.** 1999. Identification of a ribosomal ATPase in *Escherichia coli* cells. Biochimie **81:**1097–1108.
12. **Labthavikul, P., P. J. Petersen, and P. A. Bradford.** 2003. In vitro activity of tigecycline against *Staphylococcus epidermidis* growing in an adherent-cell biofilm model. Antimicrob. Agents Chemother. **47:**3967–3969.
13. **Laemmli, U. K.** 1970. Cleavage of structural proteins during the assembly of the head of bacteriophage T4. Nature **227:**680–685.
14. **McAleese, F., P. Petersen, A. Ruzin, P. M. Dunman, E. Murphy, S. J. Projan, and P. A. Bradford.** 2005. A novel MATE family efflux pump contributes to the reduced susceptibility of laboratory-derived *Staphylococcus aureus* mutants to tigecycline. Antimicrob. Agents Chemother. **49:**1865–1871.
15. **McMartin, C., and R. S. Bohacek.** 1997. QXP: powerful, rapid computer algorithms for structure-based drug design. J. Comput. Aided Mol. Des. **11:**333–344.
16. **McMurry, L. M., and S. B. Levy.** 2000. Tetracycline resistance in gram-positive bacteria, p. 660–677. *In* V. A. Fischetti, R. P. Novick, J. J. Ferretti, D. A. Portnoy, and J. I. Rood (ed.), Gram-positive pathogens. ASM Press, Washington, D.C.
17. **Moazed, D., S. Stern, and H. F. Noller.** 1986. Rapid chemical probing of conformation in 16 S ribosomal RNA and 30 S ribosomal subunits using primer extension. J. Mol. Biol. **187:**399–416.
18. **Murphy, T. M., J. M. Deitz, P. J. Petersen, S. M. Mikels, and W. J. Weiss.** 2000. Therapeutic efficacy of GAR-936, a novel glycylcycline, in a rat model of experimental endocarditis. Antimicrob. Agents Chemother. **44:**3022–3027.
19. **Petersen, P. J., and P. A. Bradford.** 2005. Effect of medium age and supplementation with the biocatalytic oxygen-reducing reagent Oxyrase on in vitro activities of tigecycline against recent clinical isolates. Antimicrob. Agents Chemother. **49:**3910–3918.
20. **Petersen, P. J., P. A. Bradford, W. J. Weiss, T. M. Murphy, P. E. Sum, and S. J. Projan.** 2002. In vitro and in vivo activities of tigecycline (GAR-936), daptomycin, and comparative antimicrobial agents against glycopeptide-intermediate *Staphylococcus aureus* and other resistant gram-positive pathogens. Antimicrob. Agents Chemother. **46:**2595–2601.
21. **Petersen, P. J., N. V. Jacobus, W. J. Weiss, P. E. Sum, and R. T. Testa.** 1999. In vitro and in vivo antibacterial activities of a novel glycylcycline, the 9-*t*-butylglycylamido derivative of minocycline (GAR-936). Antimicrob. Agents Chemother. **43:**738–744.
22. **Pioletti, M., F. Schlunzen, J. Harms, R. Zarivach, M. Gluhmann, H. Avila, A. Bashan, H. Bartels, T. Auerbach, C. Jacobi, T. Hartsch, A. Yonath, and F. Franceschi.** 2001. Crystal structures of complexes of the small ribosomal subunit with tetracycline, edeine and IF3. EMBO J. **20:**1829–1839.
23. **Rasmussen, B. A., Y. Gluzman, and F. P. Tally.** 1994. Inhibition of protein synthesis occurring on tetracycline-resistant, TetM-protected ribosomes by a novel class of tetracyclines, the glycylcyclines. Antimicrob. Agents Chemother. **38:**1658–1660.
24. **Rush, T. S., III, E. Manas, G. Tawa, and J. Alvarez.** 2005. Solvation-based scoring for high throughput docking, p. 249–273. *In* J. Alvarez and B. Shoichet (ed.), Virtual screening in drug discovery. CRC Press, Boca Raton, Fla.
25. **Ruzin, A., D. Keeney, and P. A. Bradford.** 2005. AcrAB efflux pump plays a role in decreased susceptibility to tigecycline in *Morganella morganii*. Antimicrob. Agents Chemother. **49:**791–793.
26. **Ruzin, A., M. A. Visalli, D. Keeney, and P. A. Bradford.** 2005. Influence of transcriptional activator RamA on expression of multidrug efflux pump AcrAB and tigecycline susceptibility in *Klebsiella pneumoniae*. Antimicrob. Agents Chemother. **49:**1017–1022.
27. **Sum, P. E., V. J. Lee, R. T. Testa, J. J. Hlavka, G. A. Ellestad, J. D. Bloom, Y. Gluzman, and F. P. Tally.** 1994. Glycylcyclines. 1. A new generation of potent antibacterial agents through modification of 9-aminotetracyclines. J. Med. Chem. **37:**184–188.

28. **Sum, P. E., and P. Petersen.** 1999. Synthesis and structure-activity relationship of novel glycylcycline derivatives leading to the discovery of GAR-936. Bioorg. Med. Chem. Lett. **9:**1459–1462.
29. **Tritton, T. R.** 1977. Ribosome-tetracycline interactions. Biochemistry **16:** 4133–4138.
30. **Visalli, M. A., E. Murphy, S. J. Projan, and P. A. Bradford.** 2003. AcrAB multidrug efflux pump is associated with reduced levels of susceptibility to tigecycline (GAR-936) in *Proteus mirabilis*. Antimicrob. Agents Chemother. **47:**665–669.
31. **Wang, J., P. Morin, W. Wang, and P. A. Kollman.** 2001. Use of MM-PBSA in reproducing the binding free energies to HIV-1 RT of TIBO derivatives and predicting the binding mode to HIV-1 RT of efavirenz by docking and MM-PBSA. J. Am. Chem. Soc. **123:**5221–5230.